JCI The Journal of Clinical Investigation

OSCAR is a collagen receptor that costimulates osteoclastogenesis in DAP12-deficient humans and mice

Alexander David Barrow, … , Yongwon Choi, John Trowsdale

J Clin Invest. 2011;121(9):3505-3516. https://doi.org/10.1172/JCI45913.

Research Article **Bone biology**

Osteoclasts are terminally differentiated leukocytes that erode the mineralized bone matrix. Osteoclastogenesis requires costimulatory receptor signaling through adaptors containing immunoreceptor tyrosine-based activation motifs (ITAMs), such as Fc receptor common γ (FcRγ) and DNAX-activating protein of 12 kDa. Identification of these ITAM-containing receptors and their ligands remains a high research priority, since the stimuli for osteoclastogenesis are only partly defined. Osteoclast-associated receptor (OSCAR) was proposed to be a potent FcRγ-associated costimulatory receptor expressed by preosteoclasts in vitro, but OSCAR lacks a cognate ligand and its role in vivo has been unclear. Using samples from mice and patients deficient in various ITAM signaling pathways, we show here that OSCAR costimulates one of the major FcRγ-associated pathways required for osteoclastogenesis in vivo. Furthermore, we found that OSCAR binds to specific motifs within fibrillar collagens in the ECM that become revealed on nonquiescent bone surfaces in which osteoclasts undergo maturation and terminal differentiation in vivo. OSCAR promoted osteoclastogenesis in vivo, and OSCAR binding to its collagen motif led to signaling that increased numbers of osteoclasts in culture. Thus, our results suggest that ITAM-containing receptors can respond to exposed ligands in collagen, leading to the functional differentiation of leukocytes, which provides what we believe to be a new concept for ITAM regulation of cytokine receptors in different tissue microenvironments.

Find the latest version:

https://jci.me/45913/pdf

OSCAR is a collagen receptor that costimulates osteoclastogenesis in DAP12-deficient humans and mice

Alexander David Barrow,[1,2] Nicolas Raynal,[3] Thomas Levin Andersen,[4] David A. Slatter,[3] Dominique Bihan,[3] Nicholas Pugh,[3] Marina Cella,[2] Taesoo Kim,[5] Jaerang Rho,[6] Takako Negishi-Koga,[7] Jean-Marie Delaisse,[4] Hiroshi Takayanagi,[7] Joseph Lorenzo,[8] Marco Colonna,[2] Richard W. Farndale,[3] Yongwon Choi,[5] and John Trowsdale[1]

[1]Department of Pathology, University of Cambridge, Cambridge, United Kingdom. [2]Washington University School of Medicine, Department of Pathology and Immunology, St. Louis, Missouri, USA. [3]Department of Biochemistry, University of Cambridge, Cambridge, United Kingdom. [4]Department of Clinical Cell Biology, University of Southern Denmark, Vejle/Lillebælt Hospital, Institute of Regional Health Services Research, Vejle, Denmark. [5]Department of Pathology and Laboratory Medicine, University of Pennsylvania School of Medicine, Philadelphia, Pennsylvania, USA. [6]Department of Microbiology, BK21 BioBC, and Graduate of Analytical Science and Technology, Chungnam National University, Yuseong-gu, Daejon, Republic of Korea. [7]Department of Cell Signaling, Tokyo Medical and Dental University, Tokyo, Japan. [8]Division of Endocrinology, Department of Medicine, University of Connecticut Health Center, Farmington, Connecticut, USA.

Osteoclasts are terminally differentiated leukocytes that erode the mineralized bone matrix. Osteoclastogenesis requires costimulatory receptor signaling through adaptors containing immunoreceptor tyrosine-based activation motifs (ITAMs), such as Fc receptor common γ (FcRγ) and DNAX-activating protein of 12 kDa. Identification of these ITAM-containing receptors and their ligands remains a high research priority, since the stimuli for osteoclastogenesis are only partly defined. Osteoclast-associated receptor (OSCAR) was proposed to be a potent FcRγ-associated costimulatory receptor expressed by preosteoclasts in vitro, but OSCAR lacks a cognate ligand and its role in vivo has been unclear. Using samples from mice and patients deficient in various ITAM signaling pathways, we show here that OSCAR costimulates one of the major FcRγ-associated pathways required for osteoclastogenesis in vivo. Furthermore, we found that OSCAR binds to specific motifs within fibrillar collagens in the ECM that become revealed on nonquiescent bone surfaces in which osteoclasts undergo maturation and terminal differentiation in vivo. OSCAR promoted osteoclastogenesis in vivo, and OSCAR binding to its collagen motif led to signaling that increased numbers of osteoclasts in culture. Thus, our results suggest that ITAM-containing receptors can respond to exposed ligands in collagen, leading to the functional differentiation of leukocytes, which provides what we believe to be a new concept for ITAM regulation of cytokine receptors in different tissue microenvironments.

Introduction

Cells of the mononuclear phagocyte system display remarkable plasticity and can differentiate into a variety of mononucleated and multinucleated cells with highly specialized effector functions, depending on the signals that they receive from their tissue microenvironment (1, 2). Osteoclasts are giant multinucleated cells derived from the cell fusion of mononuclear phagocyte precursors. The resorptive activity of osteoclasts is essential for bone remodeling (3) but is also responsible for the pathological bone loss observed in autoimmune diseases, such as osteoporosis and rheumatoid arthritis, and bone cancers and rare clinical disorders, such as Nasu-Hakola (NH) disease (4–6). Osteoclast differentiation is induced by the RANKL cytokine (7, 8) and costimulatory signals generated by the transmembrane immunoreceptor tyrosine-based activation motif (ITAM) adaptors, DNAX-activating protein of 12 kDa (DAP12) and Fc receptor common γ (FcRγ) (refs. 9 and 10 and Supplemental Figure 1; supplemental material available online with this article; doi:10.1172/JCI45913DS1). RANK and ITAM signaling have been shown to cooperate to induce the master transcription factor for osteoclastogenesis, NFATc1 (11). The induction of NFATc1 is thought to be dependent on the calcium signals generated by ITAM adaptor signaling, which are linked to RANK signaling by Tec family kinases (12, 13). How are the costimulatory signals generated during osteoclastogenesis? DAP12 and FcRγ signal via ITAMs encoded in their cytoplasmic tails but have short extracellular domains with no ligand-binding capacity. Therefore, DAP12 and FcRγ must associate with a ligand-binding immunoreceptor subunit in order to transduce the ITAM signals that are required to synergize with RANK signaling in osteoclastogenesis (Supplemental Figure 1). Identification of the various DAP12- and FcRγ-associated immunoreceptors and their native ligands, which can exclusively deliver the costimulatory ITAM signals for osteoclastogenesis in vivo, is currently incomplete but is crucial to our understanding of how ITAMs can mediate osteoclast differentiation during skeletal development, bone remodeling, and in bone diseases, such as NH (9, 10, 14–16).

Osteoclast-associated receptor (OSCAR) is specifically expressed by preosteoclasts and signals via FcRγ (ref. 17 and Supplemental Figure 1). OSCAR was shown to be a potent costimulatory receptor in vitro (18). However, the identity of an OSCAR ligand and the role of OSCAR in vivo has been obscure. An OSCAR ligand has been reported to be associated with osteoblast (OB) lineage cells (9, 18), which rescued *DAP12*$^{-/-}$ osteoclastogenesis in vitro (9). In mice, *Oscar* is a

Authorship note: Richard W. Farndale, Yongwon Choi, and John Trowsdale are co–senior authors.

Conflict of interest: The OSCAR-specific and mutant collagen peptides form the basis of UK patent no. 0818273.5, filed by Cambridge Enterprises Ltd. on behalf of Alexander Barrow, Richard Farndale, and John Trowsdale.

Citation for this article: *J Clin Invest.* 2011;121(9):3505–3516. doi:10.1172/JCI45913.

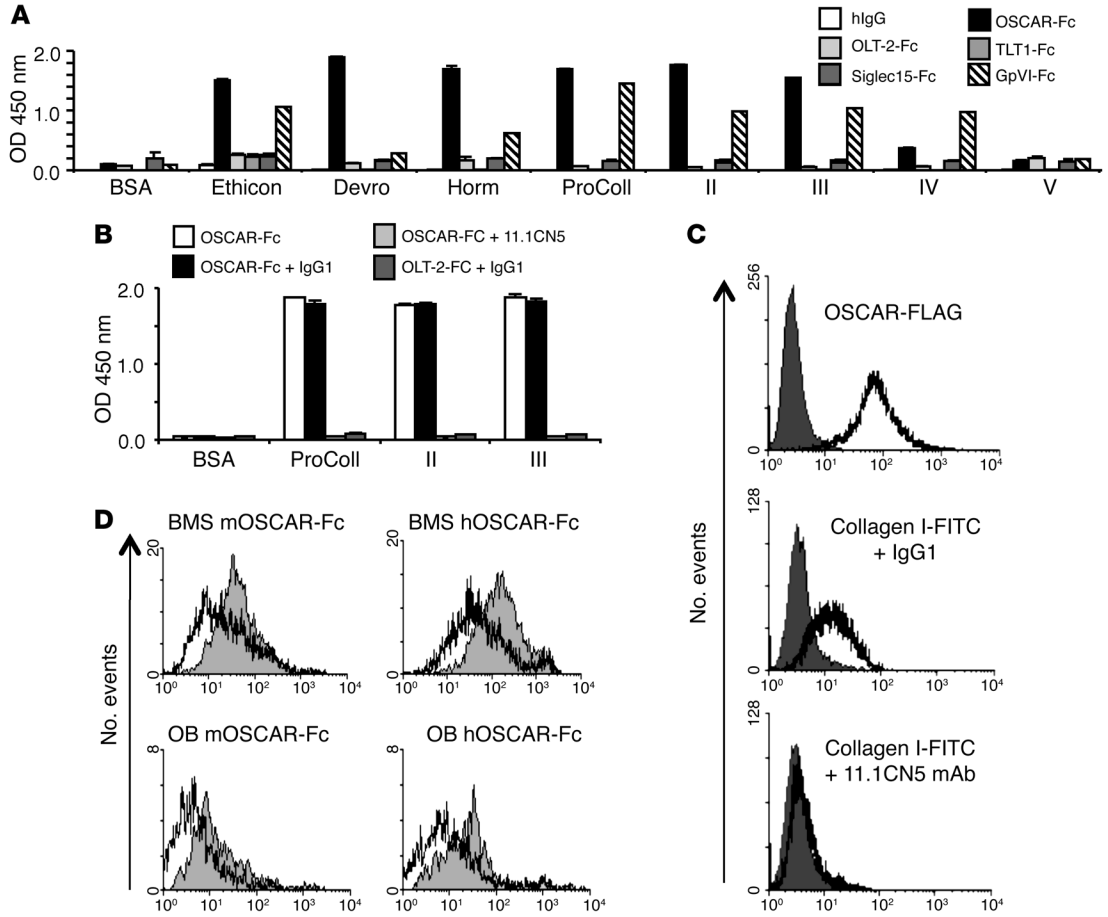

Figure 1

OSCAR is a collagen receptor. (**A**) Binding of human Ig-like receptor Fc fusions to BSA or collagens I–V in a solid-phase binding assay (see Methods). A GpVI Fc-fusion protein (GpVI-Fc) was used as positive control for collagen-binding activity, and human IgG (hIgG) was used as negative control. For a description of the other human Ig-like receptor Fc-fusion negative controls, please see Methods and Supplemental Figure 2A. (**B**) hOSCAR-Fc, preincubated with murine IgG1 or anti-hOSCAR mAb 11.1CN5, binding to BSA or collagen I–III. Solid-phase assay binding data are represented as mean ($n = 3$) ± SEM. (**C**) Collagen I–FITC binds to hOSCAR-expressing RBL-2H3 cells (clone 9). RBL-2H3 cells stably expressing hOSCAR-FLAG (white) and untransfected RBL-2H3 cells (dark gray) were stained with FITC-conjugated anti-FLAG mAb and analyzed by flow cytometry. Collagen I–FITC binding to hOSCAR-FLAG transfected RBL-2H3 cells compared with that of untransfected-RBL-2H3 cells. Preincubation with mouse anti-hOSCAR mAb 11.1CN5, but not a mouse IgG1 isotype control mAb, blocks collagen I–FITC binding to hOSCAR-FLAG expressing RBL-2H3 cells. (**D**) An OSCAR ligand is associated with OBs and stromal cells. Murine OSCAR-Fc (mOSCAR-Fc) and hOSCAR-Fc binding to collagenase-treated (white) or untreated (gray) BMSs or OBs.

RANKL-inducible gene and is thus expressed during the later stages of preosteoclast maturation (18). Mononuclear osteoclast precursors are delivered to bone surfaces where RANKL is abundantly expressed (Supplemental Figure 1 and ref. 19). Native bone surfaces are coated with a mantle of fibrillar collagen (20–22), which is expressed, and in turn covered by bone-lining cells of the OB lineage (23–25).

Collagen is an ECM protein defined by repeating (Gly-X-X′) motifs, where X is commonly proline (Pro, P) and X′ is commonly hydroxyproline (Hyp, O), a structure that promotes triple-helix formation (26). About 50 genes encode polypeptides that combine to form the 30 or so triple-helical collagens found in vertebrates. We reasoned that the OSCAR ligand might be an ECM collagen either associated with osteoblastic bone-lining cells (23–25) or exposed on native bone surfaces where osteoclasts undergo terminal differentiation in vivo (20–24, 27). This process might resemble the way exposed subendothelial collagens stimulate platelet activation through the related glycoprotein VI–FcRγ (GpVI-FcRγ) receptor, leading to thrombus formation (28). In addition, since OSCAR specifically signals via FcRγ, we reasoned that OSCAR may contribute to osteoclastogenesis in conditions in which DAP12 signaling was deficient (9, 10, 14, 16). We therefore set out to screen collagens as putative OSCAR ligands and to define the role of OSCAR as a costimulatory receptor for osteoclastogenesis in DAP12-deficient conditions.

Results

OSCAR is a receptor for ECM collagens. We used a human OSCAR-Fc (hOSCAR-Fc) fusion protein to assay for collagen-binding activity. hOSCAR-Fc bound strongly to collagens I, II, and III, weakly to collagen IV, but not to collagen V (Figure 1A). hOSCAR-Fc did not bind to the triple-helical peptide ligands for integrin $\alpha_2\beta_1$ (GFOGER and derivatives; ref. 29); the GpVI ligand, $(GPO)_{10}$, or the control peptide, $(GPP)_{10}$ (ref. 30 and Supplemental Figure 2B); or to the ECM proteins,

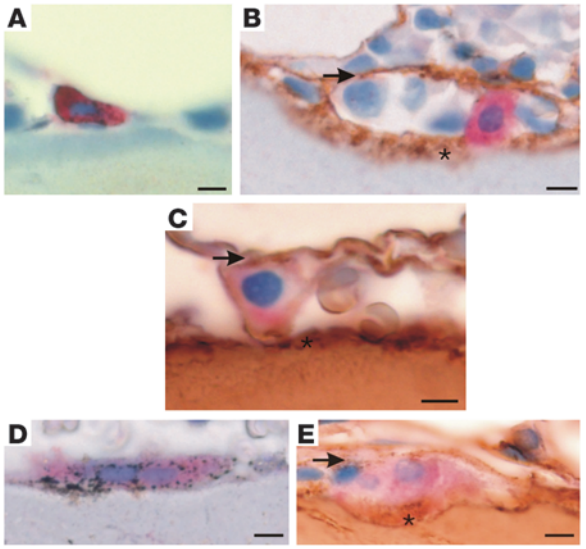

Figure 2
Collagens are exposed to preosteoclasts at bone-remodeling sites. (**A**) OSCAR (red) is specifically localized in mononuclear cells expressing TRAP (black) on bone surfaces (light blue counterstain). (**B**) Mononuclear OSCAR$^+$ cells (red) in contact with collagen III (brown) and (**C**) collagen I (brown) at bone-remodeling sites. (**D**) Multinucleated TRAP$^+$ cells express OSCAR, which (**E**) is also located in contact with collagen I at the bone surface. Note the 2 situations in which collagen I and III make contacts with OSCAR$^+$ cells: (a) located below OSCAR$^+$ cells, exposed on bone surfaces (asterisks), and also (b) above OSCAR$^+$ cells, associated with bone-lining cells (arrows) at bone-remodeling sites. The localization of each antigen was validated with 2 independent antibodies. Scale bar: 10 μm.

vitronectin or fibronectin (Supplemental Figure 2C). An anti-hOSCAR mAb (17) blocked hOSCAR-Fc binding to collagen I, II, and III (Figure 1B), showing a specific recognition of collagen by hOSCAR. FITC-conjugated collagen I also bound to hOSCAR-expressing RBL-2H3 cell clones, and this binding was also blocked by anti-hOSCAR mAb (Figure 1C and Supplemental Figure 2D). Consistent with the association of an OSCAR ligand with OB lineage or stromal cells (9, 18, 21, 23–25, 27), collagenase treatment of bone marrow stromal cells (BMSs) and calvarial OBs removed their ability to bind mouse OSCAR-Fc and hOSCAR-Fc, as assessed by immunostaining (Figure 1D). These results show that OSCAR binds to collagens I–III in vitro and to collagens associated with OB lineage or stromal cells.

Collagens are exposed to OSCAR-expressing mononuclear cells on native bone surfaces. The surface of native bone is coated with fibrillar collagen (20, 22), which is normally concealed beneath the layer of osteoblastic bone-lining cells that have expressed the collagen (21, 23, 25). We therefore investigated whether the fibrillar collagen present on bone surfaces would be exposed to mononuclear osteoclast precursors expressing OSCAR at physiological sites of osteoclast maturation and terminal differentiation in vivo. Consistent with previous reports, we found that collagens I and III were located on nonquiescent bone surfaces (20–25) and that these collagens were exposed to mononuclear cells expressing both OSCAR and the osteoclast-specific isoform of tartrate-resistant acid phosphatase (TRAP) in human bone biopsies (Figure 2, A–E). We conclude that mononuclear OSCAR$^+$ osteoclast precursors are either exposed to collagen I and III, which are both OSCAR ligands, on collagen-coated bone surfaces (20, 22) or associated with osteoblastic bone-lining cells (21, 23–25, 27) in which osteoclasts undergo terminal differentiation in vivo (19, 23, 24, 27).

OSCAR binds to a specific motif in collagens. To identify an OSCAR-binding sequence in collagen, we used overlapping triple-helical peptide libraries encompassing the entire collagen II and III sequences (Toolkits), which have been described before (29, 30). hOSCAR-Fc bound several peptides from Toolkits II and III (Figure 3A). A preliminary consensus triple-helical hOSCAR-binding sequence, GPOGPAGFOGAO, was deduced by aligning the 6 peptides that bound most strongly to hOSCAR-Fc (Figure 3B). Peptide III-36 derivatives (Supplemental Table 1) containing this motif bound hOSCAR-Fc strongly (Figure 3C). An alanine scan performed through the variable X and X′ positions of one such GXX′ polymer (Supplemental Table 1) demonstrated that hOSCAR-Fc binding required hydroxyproline at position 3 and phenylalanine at position 8 (Figure 3C). Truncation of the C-terminal triplet (GAO) from the putative motif had no effect, and, using additional amino acid substitutions, we explored the side chain determinants of hOSCAR-Fc binding (Figure 3D). This established GPOGPX′GFX′ as a minimal hOSCAR-binding triple-helical peptide (OSC^{pep}) sequence (Figure 3E). The interaction of OSCAR with OSC^{pep} was dissociable within the 1- to 10-M range (Supplemental Figure 3).

Binding of a triple-helical collagen motif to OSCAR induces signaling. We next assessed whether binding of collagen or OSC^{pep} to OSCAR could induce intracellular signaling. For this purpose, we generated human OSCAR-CD3ζ (hOSCAR-CD3ζ) nuclear factor of activated T cells–GFP (NFAT-GFP) reporter cells, which express GFP upon ligand binding to OSCAR and activation of NFAT signaling via the CD3ζ cytoplasmic signaling domain (31). GFP was expressed when hOSCAR-CD3ζ reporter cells were cultured on immobilized collagens I, II, III, or OSC^{pep} recognized by hOSCAR-Fc (Figure 4A). GFP expression was not observed after culture of hOSCAR-CD3ζ reporter cells on plates coated with BSA or collagens IV or V; control triple-helical peptide, $(GPP)_{10}$; or other triple-helical peptides that did not bind hOSCAR-Fc (Figure 4A). Crucially, hOSCAR-CD3ζ and murine OSCAR-CD3ζ reporter cells did not express GFP in response to an immobilized linear peptide (Supplemental Table 1) comprising the minimal OSC^{pep} motif (Figure 4B), showing that the triple-helical conformation of collagen is crucial for OSCAR recognition and signaling. We also screened the hOSCAR-CD3ζ reporter cells against the collagen Toolkits II and III (Supplemental Figure 4). GFP signaling generally paralleled hOSCAR-Fc binding activity (Figure 3A). We next assessed whether OSC^{pep} could induce signaling in primary cells that express OSCAR. The frequency of calcium oscillations in human monocytes cultured on immobilized OSC^{pep} was increased compared with those cultured on immobilized $(GPP)_{10}$ (Figure 4, C and D). These data show that intracellular signaling is induced upon recognition of a triple-helical collagen motif by OSCAR.

The OSCAR-binding collagen motif costimulates osteoclastogenesis. We next sought to confirm a role for OSCAR and its collagen ligand in the costimulation of osteoclastogenesis in tissue samples ex vivo (9, 10). Osteoclastogenesis from normal donor monocytes was enhanced on plate-immobilized OSC^{pep}, $(GPP)_5$-GPOGPAGFOGAO-$(GPP)_5$ and $(GPP)_5$-GAOGPAGFA-$(GPP)_5$, compared with that on immobilized BSA or control peptides that did not bind OSCAR (Figure 5, A and B). The enhanced osteoclastogenesis was inhibited when cultures were treated with hOSCAR-blocking mAb (Figure 5C), showing that the costimulatory signaling effect of OSC^{pep} on osteoclastogenesis was hOSCAR specific. Osteoclastogenesis was also increased in wild-type mouse bone marrow

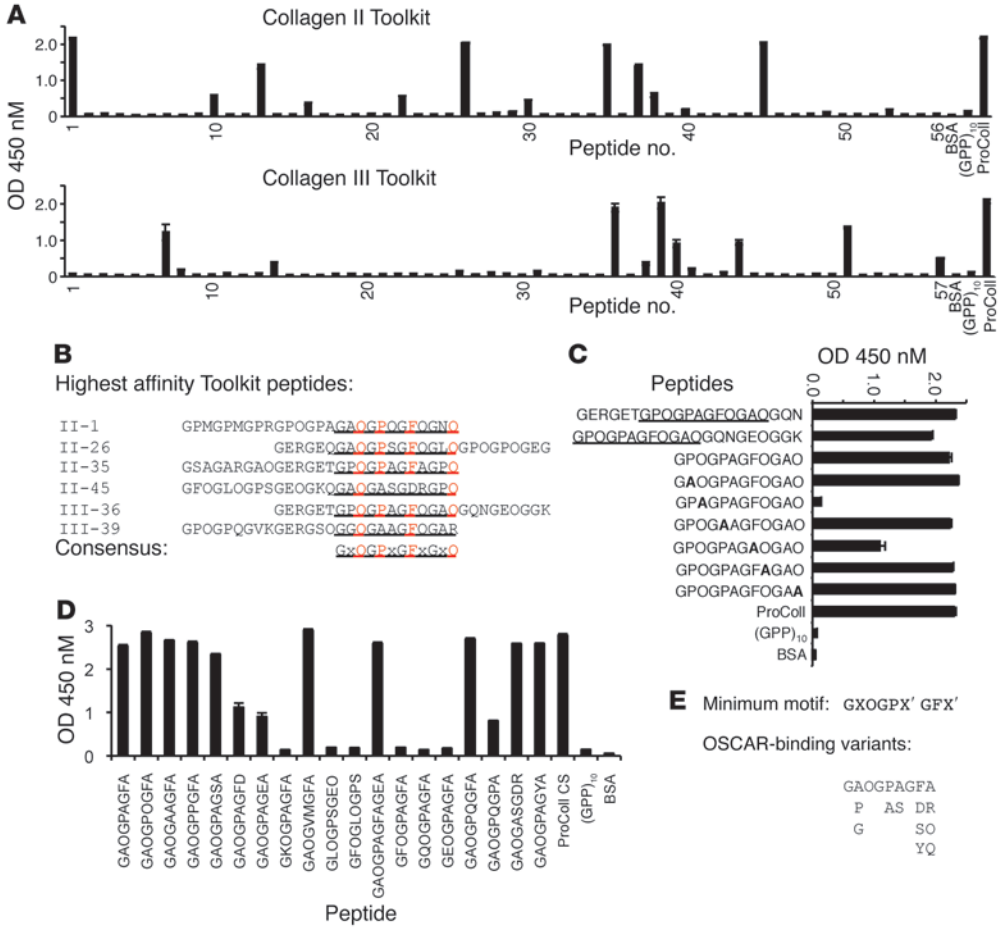

Figure 3

OSCAR binds to a specific triple-helical motif in collagen. (**A**) hOSCAR-Fc binding (*y* axis, OD 450 nM) to overlapping triple-helical peptides (*x* axis) from the collagen II and III Toolkits (29, 30). (**B**) Alignment of triple-helical collagen peptide sequences from Toolkits II and III, displaying highest affinity for hOSCAR-Fc. Predicted hOSCAR collagen-binding consensus is denoted by underlining. Alignment anchor residues are in red. (**C**) hOSCAR-Fc binding to triple-helical III-36 peptide "halves," trimmed consensus (underlined), and effect of Alanine scan (bold) through variable X and X′ residues. (**D**) Effect of various amino acid substitutions through the variable X and X′ residues of the III-36 triple-helical peptide backbone and deletion of the C-terminal triplet on hOSCAR-Fc binding. These data indicate that GPOGPX′GFX, where each proline residue can be substituted by Alanine, is a preferred generic OSCAR-binding motif. Other permissive substitutions remain to be defined. (**E**) "Minimum" collagen-binding consensus, with alignment of variant hOSCAR-binding residues. Data are represented as mean (n = 3) ± SEM.

macrophages (BMMs) cultured on immobilized OSC^{pep} compared with that in either *Oscar*$^{-/-}$ or *Fcer1g*$^{-/-}$ BMMs (Figure 6, A and B). Expression of the osteoclast-specific genes *TRAP*, cathepsin K (*Ctsk*), calcitonin receptor (*Calcr*), and *Nfatc1* was increased in wild-type BMMs cultured on OSC^{pep} compared with those cultured on BSA, but this was not observed in *Oscar*$^{-/-}$ BMM cultures cultured on either BSA or OSC^{pep} (Figure 6C). These results show that binding of the collagen motif to OSCAR evoked specific FcRγ signaling (17) in preosteoclasts, which costimulated osteoclastogenesis.

The effects of TGF-β1 and OSC^{pep} on osteoclastogenesis are additive. TGF-β1 is a known enhancer of RANKL action. We next assessed whether the combined effects of immobilized OSC^{pep} and TGF-β1 had an additive effect for osteoclastogenesis. We compared osteoclastogenesis of wild-type and *Oscar*$^{-/-}$ BMMs cultured on either immobilized BSA or OSC^{pep}, with or without TGF-β1. In the presence of TGF-β1, osteoclastogenesis of wild-type and *Oscar*$^{-/-}$ BMMs cultured on BSA was enhanced, although no differences were observed between genotypes (Figure 7). TGF-β1 markedly increased the number of giant TRAP^{+} osteoclasts for wild-type BMMs cultured on immobilized OSC^{pep} compared with those cultured on BSA. However, this was not observed for *Oscar*$^{-/-}$ BMMs, showing the effects of OSC^{pep} on osteoclastogenesis were OSCAR specific and additive with TGF-β1 (Figure 7).

OSCAR recognition of its collagen motif costimulates osteoclastogenesis from DAP12-deficient mice and patients with NH ex vivo. NH disease results from a genetic deficiency in the DAP12 costimulatory pathway of osteoclastogenesis (5, 32). An intriguing discovery was that monocytic osteoclast precursors from triggering receptor expressed on myeloid cells 2–deficient (TREM-2–deficient) or DAP12-deficient patients with NH have impaired osteoclast differentiation when cultured with recombinant RANKL in vitro (14, 16). However, patients with NH are not deficient in osteoclast differentiation in vivo and can present with an osteoporotic bone phenotype, which is characterized by trabecular bone loss in addition to bone cysts (5). DAP12-independent costimulatory pathways for osteoclastogenesis must therefore be operating in the pathogenesis of NH bone

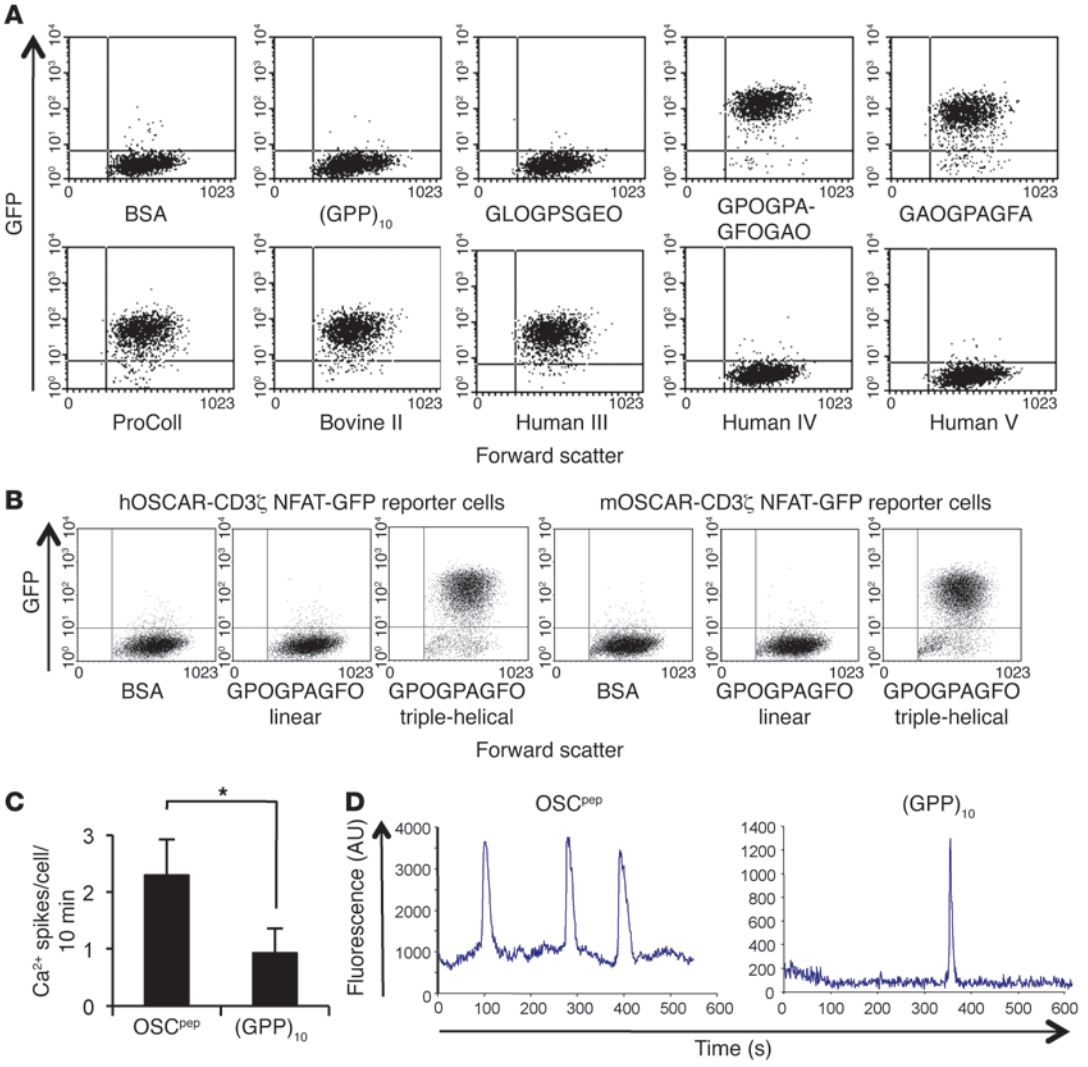

Figure 4

The triple-helical conformation of the OSCAR-binding motif in collagen ligands can induce OSCAR signaling. (**A**) Dot plots (2,000 events) displaying the response of a hOSCAR-CD3ζ NFAT-GFP reporter cell line to immobilized BSA, $(GPP)_{10}$, $(GPP)_5$-GLOGPSGEO-$(GPP)_5$, $(GPP)_5$-GPOGPAGFOGAO-$(GPP)_5$, or $(GPP)_5$-GAOGPAGFA-$(GPP)_5$ or collagens I–V (*y* axis, GFP expression; *x* axis, forward scatter). (**B**) Dot plots (10,000 events) displaying the responses (GFP expression) of the hOSCAR-CD3ζ and murine OSCAR-CD3ζ (mOSCAR-CD3ζ) NFAT-GFP reporter cell lines to immobilized BSA; a linear peptide containing the minimal OSCAR-binding sequence GPOGPAGFO (linear); or a triple-helical peptide designed to the minimal OSCAR-binding sequence, $(GPP)_5$-GPOGPAGFO-$(GPP)_5$ (peptide sequences can be found in Supplemental Table 1) (*y* axis, GFP expression; *x* axis, forward scatter). (**C**) Calcium spikes per cell per 10-minute period for human monocytes cultured on either immobilized OSC^{pep} or $(GPP)_{10}$. Data are represented as mean ($n = 5$) ± SEM; $^*P < 0.05$. (**D**) Representative calcium traces for human monocytes cultured on either immobilized OSC^{pep} or $(GPP)_{10}$.

disease, most likely through alternative FcRγ-mediated pathways (9, 10). For example, DAP12-deficient osteoclastogenesis in vitro can be rescued in coculture with OBs because of the association of an OSCAR ligand with these cells (refs. 9 and 18 and Figure 1D). Hence, we assessed whether immobilized OSC^{pep} could provide an alternative differentiation signal to rescue osteoclastogenesis from *DAP12*$^{-/-}$ BMMs in vitro, as might be expected in vivo (20–25, 27) or in cocultures with OBs in vitro (9, 18). Immobilized OSC^{pep} rescued the in vitro osteoclastogenesis defect of murine *DAP12*$^{-/-}$ BMMs (Figure 8A). The rescued giant multinuclear *DAP12*$^{-/-}$ cells stained for TRAP (Figure 8B) and formed well-defined actin-rich podosome belts (Figure 8C). These results show that the OSCAR-binding collagen motif can costimulate DAP12-deficient osteoclastogenesis.

To prove that the costimulatory signals elicited by the triple-helical collagen peptides that rescued DAP12-deficient osteoclastogenesis in preosteoclast cultures were OSCAR specific, we compared osteoclastogenesis of BMMs from *DAP12*$^{-/-}$*Oscar*$^{-/-}$ and *DAP12*$^{-/-}$ mice in culture with plate-immobilized OSC^{pep}. *DAP12*$^{-/-}$, but not *DAP12*$^{-/-}$*Oscar*$^{-/-}$, BMM precursors developed giant $TRAP^+$ multinucleated cells in response to RANKL when cultured on immobilized OSC^{pep} (Supplemental Figure 5, A–C). This effect was OSCAR specific, because osteoclastogenesis on immobilized OSC^{pep} was restored by retroviral transduction of *DAP12*$^{-/-}$*Oscar*$^{-/-}$ BMMs with murine OSCAR (Figure 8D and Supplemental Figure 6, A and B) or DAP12 (Supplemental Figure 6, C and D). Giant $TRAP^+$ multinuclear cells also developed on immobilized $(GPP)_{10}$ in the presence of

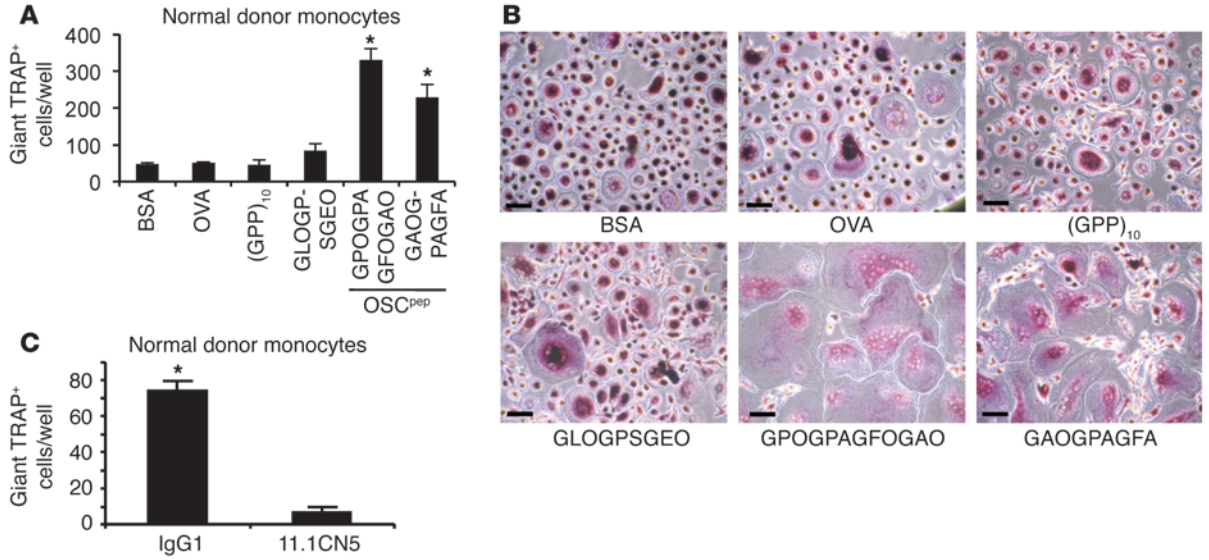

Figure 5

The OSCAR collagen-binding motif costimulates osteoclastogenesis from human monocytes. (**A**) Day 6 RANKL differentiation of human monocytes on the plate-immobilized OSC^{pep}, $(GPP)_5$-GPOGPAGFOGAO-$(GPP)_5$, or $(GPP)_5$-GAOGPAGFA-$(GPP)_5$, or the control protein BSA, or the control peptides OVA or $(GPP)_{10}$ or $(GPP)_5$-GLOGPSGEO-$(GPP)_5$. Data are represented as mean (n = 3) ± SEM; *P < 0.05 indicates an increase in osteoclasts cultured on OSC^{pep} compared with other culture conditions. (**B**) TRAP staining of day 6 human osteoclast cultures. Scale bar: 70 μM. (**C**) Anti-hOSCAR mAb 11.1CN5, but not IgG1, inhibits osteoclastogenesis on immobilized OSC^{pep}, showing the costimulatory action of OSC^{pep} on osteoclastogenesis is hOSCAR specific. Data are represented as mean (n = 3) ± SEM; *P < 0.05.

RANKL but to a lesser extent (Figure 8D and Supplemental Figure 6, A and B), which likely resulted from the retroviral overexpression of mouse OSCAR (Supplemental Figure 6E).

To further evaluate the significance of these findings in a clinical setting, we also assessed whether OSC^{pep} could costimulate osteoclastogenesis using monocytes from TREM-2– or DAP12-deficient patients with NH (14, 16). Greater numbers of $TRAP^+$ multinucleated cells were formed when either TREM-2– or DAP12-deficient monocytes from patients with NH were cultured with RANKL on immobilized OSC^{pep}, compared with those cultured on BSA or $(GPP)_{10}$ (Figure 8, E–G). Thus, data from both mouse and NH samples showed that OSCAR recognition of its triple-helical collagen motif can costimulate osteoclastogenesis independently of TREM-2 and DAP12 signaling.

OSCAR costimulates DAP12-deficient osteoclastogenesis in vivo. Since OSCAR costimulated osteoclastogenesis independently of TREM-2 and DAP12 signaling in vitro, we sought to confirm a role for OSCAR in osteoclast differentiation in vivo. Since we cannot knockout, knockdown, or mutate all of the motifs in all of the collagens that OSCAR binds, we chose to investigate OSCAR deficiency in vivo. However, *Fcer1g*$^{-/-}$ mice do not show any apparent defect in bone, consistent with the known biological redundancy with the DAP12 pathway of osteoclastogenesis (9, 10). Consistent with this, *Oscar*$^{-/-}$ mice did not show any difference in bone volume when compared to wild-type mice (data not shown). However, when we generated *DAP12*$^{-/-}$*Oscar*$^{-/-}$ mice, they showed decreased $TRAP^+$ osteoclast numbers (Figure 9, A and B), decreased osteoclast size (Figure 9C), and a reduction in eroded bone surfaces (Figure 9D) compared with those of *DAP12*$^{-/-}$ mice. Consistent with these data, OSCAR deletion caused reciprocal changes in marrow space and trabecular bone in *DAP12*$^{-/-}$*Oscar*$^{-/-}$ mice compared with those of *DAP12*$^{-/-}$ mouse bone (Figure 9A, toluidine blue and von Kossa, and Figure 9E). OB numbers and bone formation parameters did not differ between the *DAP12*$^{-/-}$*Oscar*$^{-/-}$ and *DAP12*$^{-/-}$ mice, showing that the differences observed were not due to defects in the OB compartment (Supplemental Figure 7, A–D). The number and volume of trabeculae in bones from *DAP12*$^{-/-}$*Oscar*$^{-/-}$ mice were also increased compared with those of *DAP12*$^{-/-}$ mice when assessed by micro-CT (μCT) (Supplemental Figure 8, A and B). These results show that OSCAR is a bona fide costimulatory receptor required for optimal osteoclastogenesis in vivo. Furthermore, they show that OSCAR costimulated an FcRγ-associated pathway for osteoclastogenesis in DAP12-deficient mice.

Discussion

The ECM is known to influence leukocyte differentiation, consistent with an effect of ITAM on cytokine receptor signaling (9, 10, 13, 33–36), and the association of growth factors with the ECM. However, there is surprisingly little evidence for ITAM receptors that can recognize ECM ligands or understanding of how the ECM might cooperate with cytokines to influence leukocyte differentiation in different tissue microenvironments. To our knowledge, by identifying OSCAR as a collagen receptor, we are the first to show a new role for the recognition of exposed ECM ligands in the ITAM-mediated costimulation of osteoclastogenesis.

We have located 6 prominent OSCAR-binding sites in collagens II and III. Of the 4 sites in collagen II, 3 share identity with collagen 1α1 and are conserved in collagen 1α2; in the fourth site, 6 out of the 9 residues are identical in collagen 1α1, and 7 out of the 9 are identical in collagen 1α2. There are also several OSCAR-binding sites of lower affinity in collagens II and III (Figure 3A). These OSCAR-binding sites would be expected to decorate the ECM surface exposed to cells expressing OSCAR, so that the cooperative binding of several copies of ligand to several copies of recep-

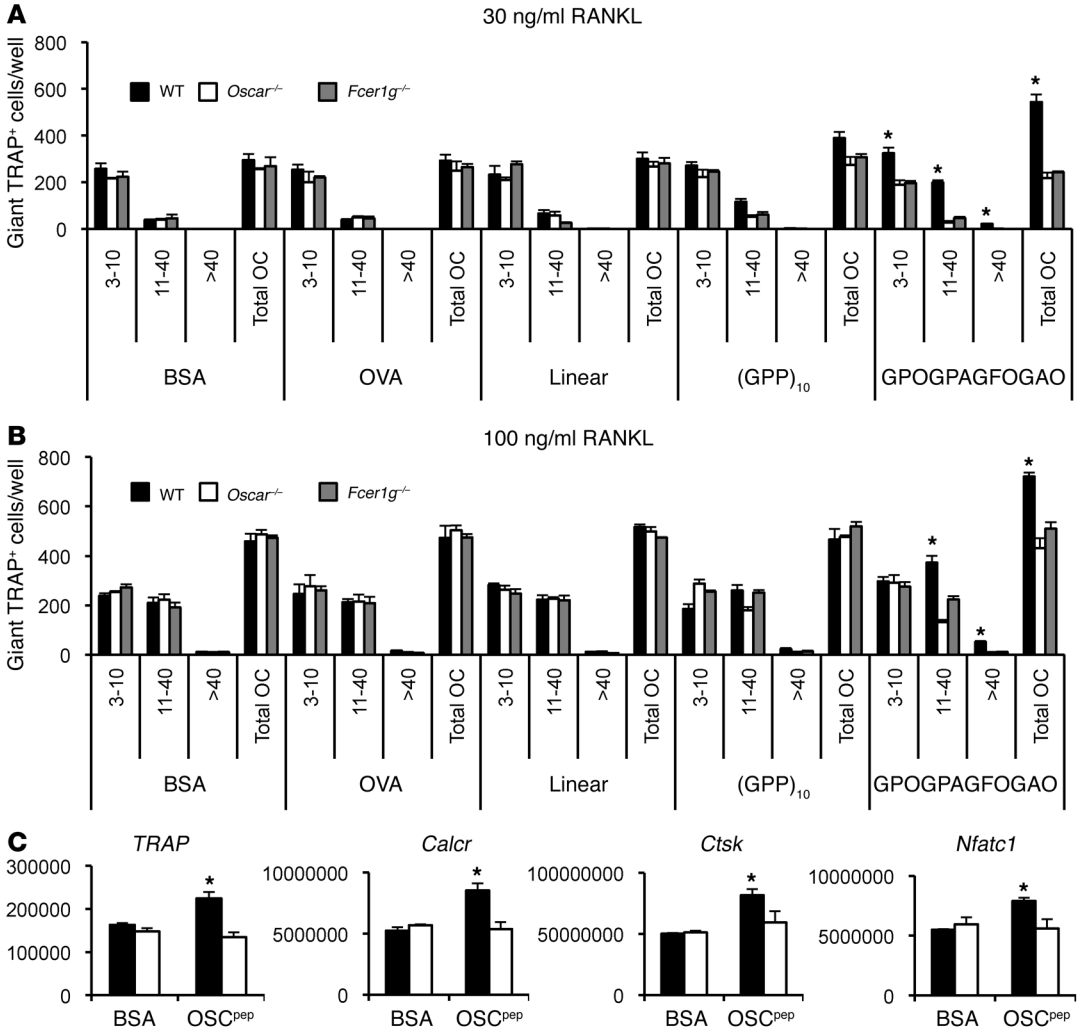

Figure 6

The OSCAR collagen-binding motif costimulates murine osteoclastogenesis. (**A**) RANKL differentiation of wild-type, *Oscar*$^{-/-}$, or *Fcer1g*$^{-/-}$ BMMs cultured on either immobilized OSC^{pep} or control proteins at 30 ng/ml RANKL or (**B**) 100 ng/ml RANKL. Data are represented as mean ($n = 3$) ± SEM; *$P < 0.05$ indicates an increase in osteoclasts cultured on OSC^{pep} compared with all other culture conditions and genotypes. The number of nuclei (e.g., 3–10, 11–40, or >40) per TRAP^{+} osteoclast (OC), as well as the total number of osteoclasts, was enumerated for each well (*x* axis). (**C**) Quantitative RT-PCR expression of osteoclast genes from day 5 osteoclast cultures (black bars, wild type; white bars, *Oscar*$^{-/-}$). Data are normalized relative to GAPDH and represented as mean ($n = 3$) ± SEM; *$P < 0.05$.

tor would lead to receptor clustering and activation. A range of intrinsic affinities of ligand in the ECM are therefore likely to be displayed, increasing the binding avidity. Thus, each type of collagen fiber has the potential to bind and cluster multiple copies of OSCAR to transduce ITAM signaling via FcRγ.

Specifically for osteoclastogenesis, we envisage that OSCAR/collagen costimulation of RANKL may be important in several situations. For example, osteoclast precursors may gain access to bone surfaces either from the bone marrow or the blood (Supplemental Figure 1). To gain access to native bone surfaces, circulating osteoclast precursors would need to undergo transendothelial migration across capillaries sheathed in collagen III (23) that express RANKL (37). Whether recruited from the circulation or directly from the marrow, preosteoclasts would still be exposed to collagen I– and collagen III–coated bone surfaces in close association with osteoblastic bone-lining cells (refs. 20–25, 27, and Figure 2). During skeletal development, the collagen I–rich mesenchyme surrounding cartilaginous bone rudiments (38) is a known site of deposition for preosteoclasts as well as along the growth plate, which also consists of type II and X cartilage (39).

It is possible that OSCAR may contribute to osteoclastogenesis in disease, such as rheumatoid arthritis (40), characterized by the exposure of epitopes in collagen, or in the pathogenesis of NH bone disease (5, 32), as an alternative FcRγ-mediated pathway of osteoclastogenesis. For example, in rheumatoid arthritis, it is possible that more OSCAR-binding motifs in collagens become exposed as proteases (e.g., upregulated MMPs) strip off any masking collagen-associated proteins. The degradation of collagen fibers might also lead to the exposure of sequences embedded within the body of the fiber. Incoming OSCAR^{+} osteoclast precursors, recruited by cytokine generation (e.g., RANKL), might then be activated by such exposed "neoepitopes." In the case of NH bone disease, we have shown that OSCAR binding to its cognate triple-helical motif in

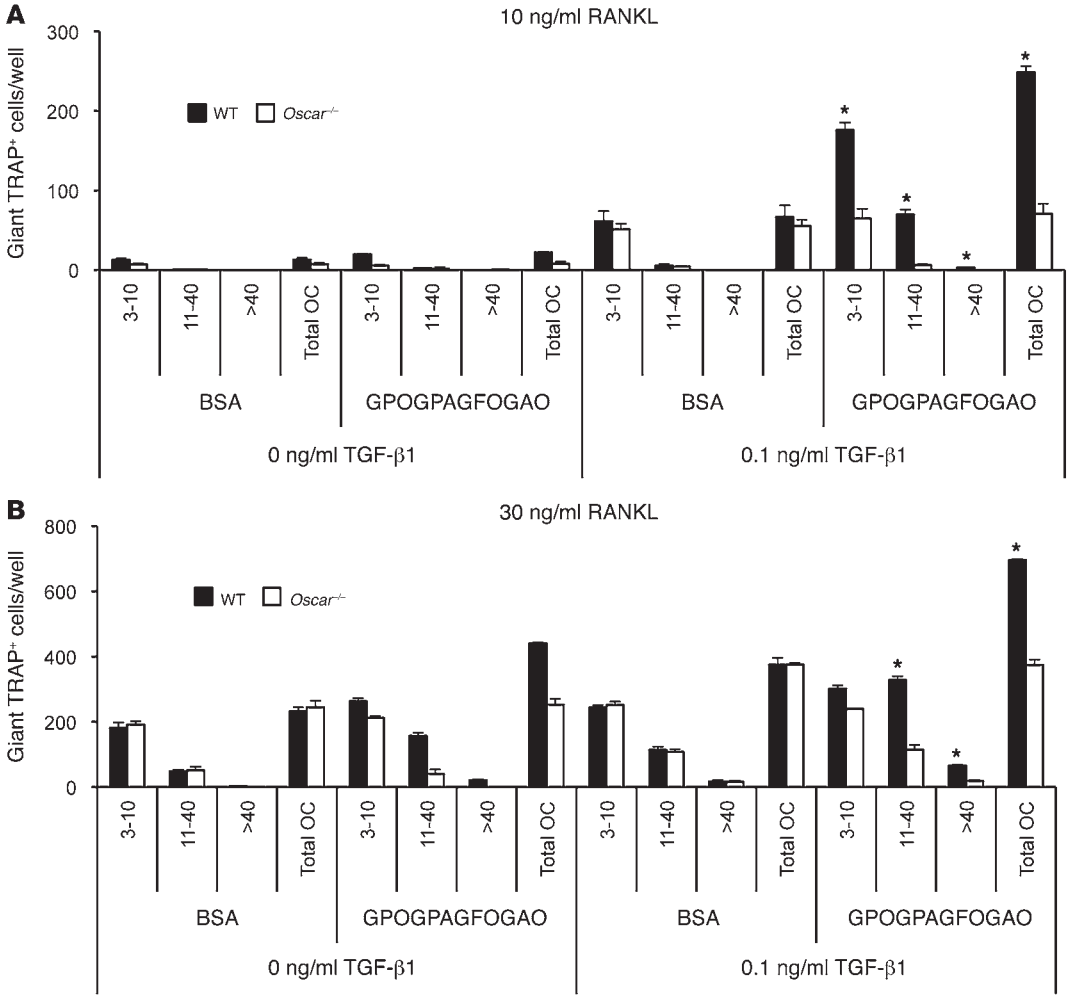

Figure 7

The effects of TGF-β1 and immobilized OSC^{pep} on osteoclastogenesis are additive. (**A**) Effect of ±0.1 ng/ml TGF-β1 on the osteoclastogenesis of wild-type or *Oscar*$^{-/-}$ BMMs cultured on either immobilized BSA or OSC^{pep} at 10 ng/ml RANKL or (**B**) 30 ng/ml RANKL. The number of nuclei (e.g., 3–10, 11–40, or >40) per TRAP^{+} osteoclast, as well as the total number of osteoclasts, was enumerated for each well (*x* axis). Data are represented as mean (n = 3) ± SEM; *P < 0.05 indicates an increase in osteoclasts cultured on OSC^{pep} plus TGF-β1 compared with either BSA with or without TGF-β1 or OSC^{pep} alone.

collagen costimulated the osteoclastogenesis of monocytes from TREM-2– and DAP12-deficient patients with NH, and the targeted genetic deletion of OSCAR in DAP12-deficient (*DAP12*$^{-/-}$*Oscar*$^{-/-}$) mice resulted in approximately 50% reduction in TRAP^{+} cells and approximately 50% increase in trabecular bone volume (as assessed by μCT), compared with those of *DAP12*$^{-/-}$ mice.

Our finding that specific collagens, normally embedded in the ECM or "hidden" from patrolling or circulating leukocytes behind a layer of bone-lining or microendothelial cells, are OSCAR ligands suggests that the revealed or exposed ECM in nonquiescent tissues plays an active role in the local ITAM-mediated regulation of osteoclastogenesis. These data suggest that other costimulatory ITAM receptors (e.g., associated with DAP12) in osteoclastogenesis might also be predicted to sense changes in, or the exposure of, local ECM in nonquiescent bone tissue. This concept may also be relevant to alternative modes of differentiation for mononuclear phagocytes, such as the synergy of DAP12 signaling with IL-4 in macrophage fusion and the formation of multinucleated giant cells (MGCs) (33). Foreign body MGCs can be formed in granulomatous disease, such as tuberculosis, in which they are associated with a restriction of the cell-to-cell spread of mycobacteria or with the surgical implantation of biomaterials (2). Local tissue damage caused by infections or invasive surgical procedures could result in exposure of ECM proteins that could be sensed by ITAM receptors, which could synergize with cytokines associated with or expressed by the perturbed tissue. Interestingly, MGCs are associated with increased MMP-9 activity, which may contribute to tissue damage by liberating proteins or factors embedded in the ECM (41). In addition to osteoclasts, human OSCAR is expressed on monocytes and macrophages as well as neutrophils and myeloid dendritic cells (17) and possibly also microglia. Thus, human OSCAR could conceivably play a wider role in the human mononuclear phagocyte system and might be predicted to synergize with IL-4 or IL-13 in MGC formation (2, 33) or possibly other cytokines and soluble factors at sites in which collagen ligands are exposed or become dysregulated, e.g., during ECM remodeling by cancers (42, 43). In this regard, collagen could be regarded as a

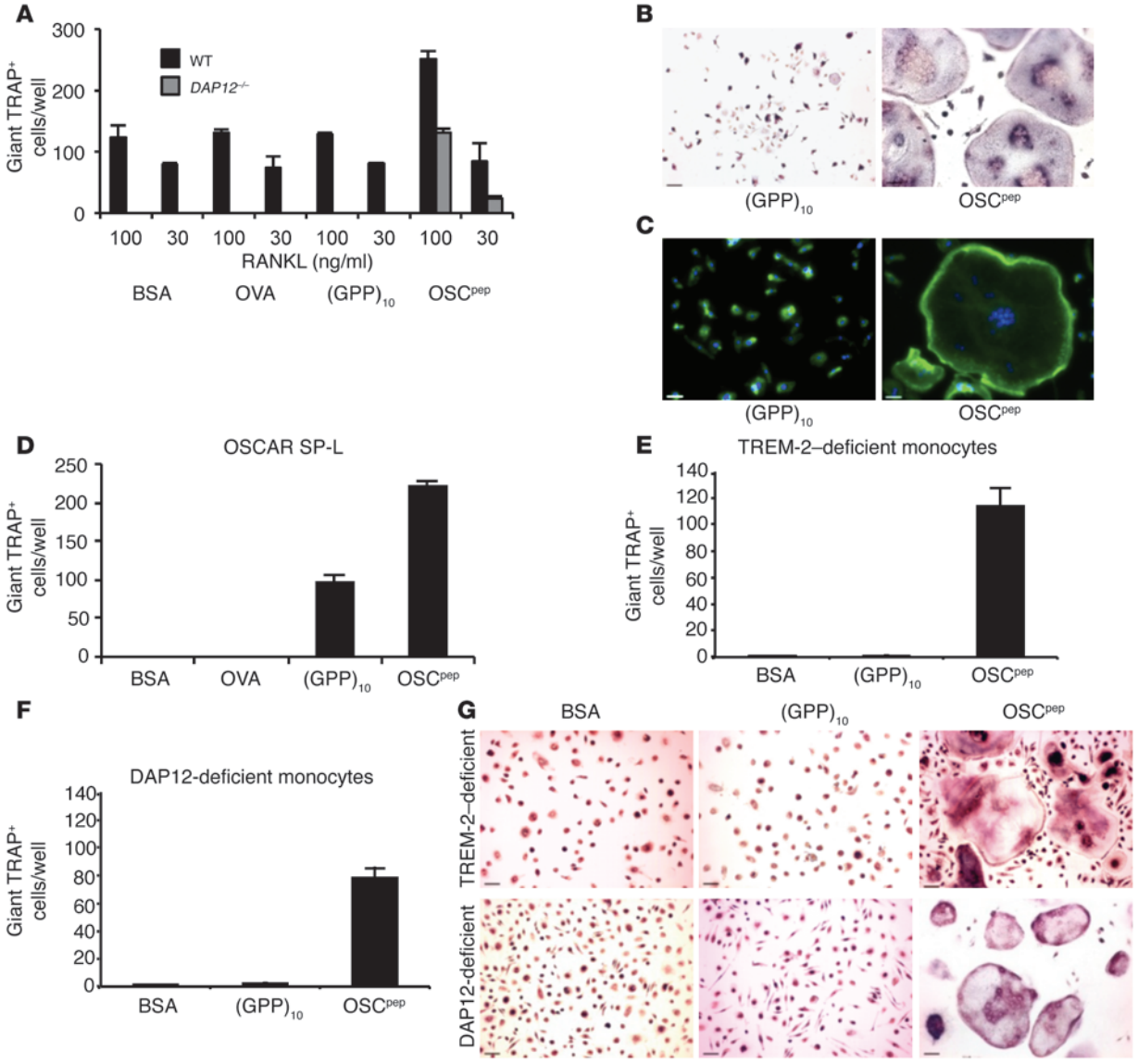

Figure 8

OSCAR recognition of the collagen motif costimulates osteoclastogenesis of precursors from *DAP12*$^{-/-}$ mice and TREM-2– and DAP12-deficient patients with NH. (**A**) Immobilized OSC^{pep} rescued the osteoclastogenesis of murine *DAP12*$^{-/-}$ BMMs (day 6) compared with that of wild-type (day 5). (**B**) TRAP staining (scale bar: 70 μM), (**C**) DAPI (blue fluorescence), and Phalloidin–Alexa Fluor 488 (green) staining of OSC^{pep}-rescued giant multinucleated *DAP12*$^{-/-}$ cells (scale bar: 60 μM). (**D**) Retroviral transduction of mouse OSCAR, long-signal peptide isoform (SP-L), rescued osteoclastogenesis of *DAP12*$^{-/-}$*Oscar*$^{-/-}$ preosteoclasts, showing that the costimulatory signaling and rescue of osteoclastogenesis is OSCAR specific. (**E**) Effect of immobilized proteins and peptides on osteoclastogenesis of TREM-2–deficient (day 14) or (**F**) DAP12-deficient monocytes from patients with NH (day 10). (**G**) TRAP staining of RANKL-differentiated NH monocytes in wells coated with different proteins and peptides (scale bar: 70 μM). Data are represented as mean (n = 3) ± SEM.

"damage-associated molecular pattern" that could be sensed by OSCAR in immune cells to detect perturbations in the local ECM.

Interestingly, receptors encoding immunoreceptor tyrosine-based inhibition motifs (ITIMs), such as PIR-B, SIRPα, and PECAM-1, can negatively regulate ITAM receptor signaling (44) through recruitment of inhibitory protein tyrosine phosphatases, such as SHP-1 and/or SHP-2, or the inositol phosphatase, SHIP (45–47). Like the RANKL-osteoprotegerin axis (3, 8), OSCAR/ITAM signaling may be negatively regulated by myeloid cell expression of the ITIM receptor, LAIR-1, which also binds to collagen and is genetically linked to OSCAR within the leukocyte receptor complex (48, 49). In the absence of OSCAR signaling, such as in *DAP12*$^{-/-}$*Oscar*$^{-/-}$ mice, LAIR-1 inhibitory signaling on preosteoclasts could negatively regulate osteoclastogenesis in which collagens are exposed, leading to a reduction in the TRAP^{+} cells, which we observed. Since murine OSCAR is RANKL-inducible (18), this might suggest that, along with a requirement for at least "2 signals" (RANKL and ITAM), preosteoclasts may be similar to other immune cells that must pass a series of checks and balances to avoid inappropriate differentiation at the "wrong tissue site," par-

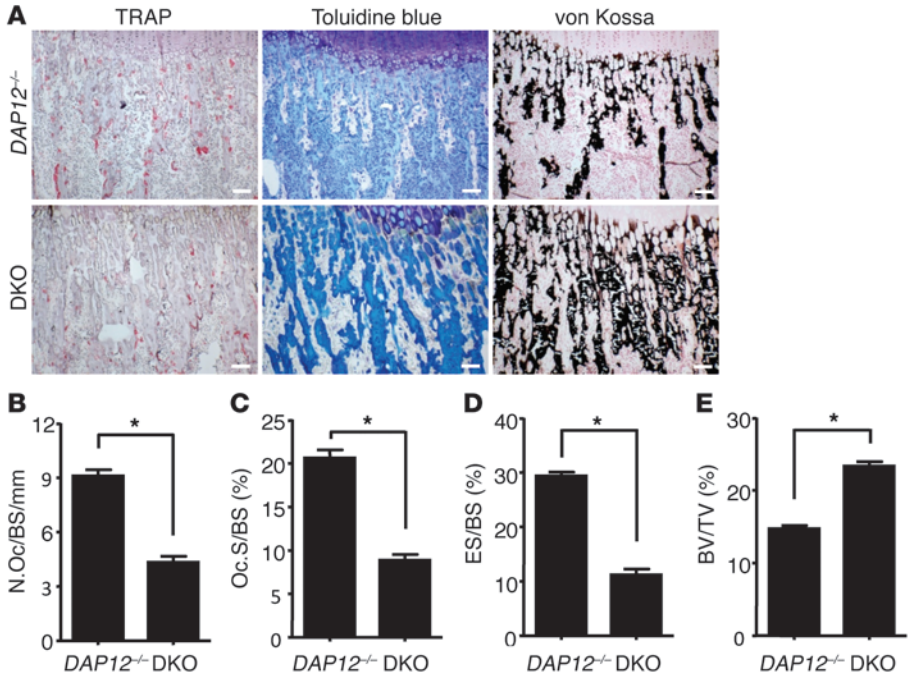

Figure 9
OSCAR costimulates a major DAP12-independent pathway for osteoclastogenesis in vivo. (**A**) Histology (TRAP, toluidine blue, and von Kossa staining) of the tibia (metaphysis) from *DAP12*$^{-/-}$*Oscar*$^{-/-}$ (DKO) and *DAP12*$^{-/-}$ mice (scale bar: 100 μM). The bone marrow cavity of *DAP12*$^{-/-}$*Oscar*$^{-/-}$ mice is reduced (toluidine blue staining) and filled with more unresorbed bone (von Kossa) compared with that of *DAP12*$^{-/-}$ mice. (**B**) Decrease in TRAP^{+} osteoclast numbers (osteoclast number/bone surface/mm [N.Oc/BS/mm]), (**C**) osteoclast size (osteoclast surface/bone surface [Oc.S/BS] [%]), and (**D**) eroded bone surfaces (eroded surface/bone surface [ES/BS]), with a concomitant increase in (**E**) trabecular bone volume (bone volume/tissue volume [BV/TV]) in *DAP12*$^{-/-}$*Oscar*$^{-/-}$ mice compared with those in *DAP12*$^{-/-}$ mice. Data are represented as mean (n = 10) ± SEM; *P < 0.05.

ticularly since RANKL is known to be expressed in tissues outside of bone (7, 8). The identification of OSCAR as a collagen receptor that can costimulate osteoclastogenesis opens the way for its exploitation for therapeutic interventions in bone metabolism. Of note, OSCAR expression is upregulated in rheumatoid arthritis (40), and polymorphisms in the OSCAR promoter are associated with low bone mineral density in postmenopausal women (50).

Methods

Collagens. Ethicon (Ethicon Corp.) and Devro (Devro) are preparations of bovine collagen I fibers. ProColl (Devro) is a collagen I monomer. Horm (Nycomed Pharma GmbH) is an equine collagen I fiber preparation. Bovine collagen II and human collagens III, IV, and V were purchased from Sigma-Aldrich.

Solid-phase assay and peptide immobilization. Peptide synthesis; polarimetric confirmation of triple-helical status; immobilization of proteins, collagens, and peptides; and the solid-phase binding assay were performed as described previously (29, 30). BSA and ovalbumin peptide SIINFEKL (OVA) were purchased from Sigma-Aldrich. Collagens, peptides, and control proteins were immobilized onto plates at concentrations of 10 μg/ml in 10 mM acetic acid. All peptides were certified LPS-free by LAL assay (Lonza).

BMS and OB culture. Adherent BMSs were flushed from the femurs and tibias of 3- to 4-week-old mice. Calvarial OBs were isolated from neonatal mice as described previously (18). BMSs and OBs were cultured in DMEM supplemented with 10% heat-inactivated fetal calf serum, 100 U/ml penicillin and streptomycin, and 100 μg/ml ascorbate. BMSs and OBs were activated with 10^{-8} M vitamin 1,25-$(OH)_2D_3$ and 10^{-6} M prostaglandin E_2 (Sigma-Aldrich). Mouse and hOSCAR-Fc binding to BMSs and OBs was assessed before and after collagenase treatment (30 minutes at 37°C) by flow cytometry. Fc-fusion proteins were detected using goat anti-human IgG-PE (Southern Biotechnologies), and mouse CD45-FITC^{+} (Southern Biotechnologies) cells were excluded by electronic gating.

Collagenase treatment. BMSs and OBs were incubated for 30 minutes with 100 U/ml chromatography-purified, tissue culture–tested *Clostridium histolyticum* collagenase type VII (Sigma-Aldrich), before staining with hOSCAR-Fc and mouse OSCAR-Fc fusion proteins and detection with goat anti-human IgG-PE (Southern Biotechnologies).

Fc fusions. Production and purification of mouse and human Ig-like receptor Fc-fusion proteins were performed as described previously (51). The GenBank accession number of the human Ig-like receptor OSCAR-like transcript–2 (OLT-2), which we believe to be novel, is DQ479398. GpVI (28), TREM-1 (51), TREM-2 (14), TREM-like transcript-1 (TLT1) (52), CRTAM (53), and Siglec-15 (54) have been described before.

mAb blocking experiments. Fc fusions (30 minutes, room temperature) or RBL-2H3 cells (30 minutes on ice) were preincubated with 2.5 μg/ml of either mouse anti-human OSCAR mAb 11.1CN5 (17) (Beckman Coulter) or IgG1 control mAb (Dako) prior to assessment by either solid-phase assay (Fc-fusions) or incubation with 5 μg/ml FITC-conjugated collagen I (collagen I–FITC). RBL-2H3 cells were washed twice in PBS, before analysis of collagen I–FITC binding by flow cytometry.

Double immunostaining of bone sections. Decalcified paraffin-embedded bone marrow biopsies from 11 healthy individuals were included in the study according to the specifications of the Danish Ethical Committee approval no. S-20070121. Sections were processed as described previously (23). Antibodies against human OSCAR were as follows: goat anti-OSCAR, N terminus sc-34230, and C terminus sc-34233 from Santa Cruz Biotechnology Inc.; against collagen type I, rabbit anti-collagen type I, ab34710 and ab292, from AbCam; against collagen type III, mouse anti-collagen type III, clone FH-7A, from AbCam and rabbit anti-collagen type III from professor Juha Risteli, University of Oulu, Oulu, Finland; and against the osteoclast-specific TRAP isoform, TRACP5b, clone ZY-9c5, from Zymed. The subsequent detection involved gold-silver enhancement for TRAPc5, Liquid Permanent Red (Dako) staining for OSCAR, and DAB staining for collagen type I and III, as described previously (23). Bone biopsies from 11 healthy patients were double stained with antibodies for either OSCAR/TRAP or OSCAR/collagen I or OSCAR/collagen III, and the colocalization of these antigens at nonquiescent bone-remodeling sites was assessed.

Plasmids. Human OSCAR was cloned into the p3xFLAG CMV-9 vector (Sigma-Aldrich), and single-cell RBL-2H3 clones were selected with 1 mg/ml active G418 (Gibco) using primers 5′-GTGTAAGCTTGACATCACTCC-

GTCTGTCCC-3′ and 5′-GCCATCTAGATTGGAAGTCTCGGGCTGCAG-3′. Primers to the extracellular domains of human, 5′-GTGTAGATCTGACATCACTCCGTCTGTCCC-3′ and 5′-CCAGGTCGACTAGGTTCCCCCGGGTGTAGT-3′, and murine, 5′-TGCAGATCTGACTTCACACCAACAGCG-3′ and 5′-ACGGTCGACGTTTCCCTGGGTATAGTCCA-3′, OSCAR were cloned into pDISPLAY (Invitrogen), a construct which encodes an N-terminal HA tag and the transmembrane domain of the PDGFR. The resulting N-terminal HA-tagged murine and human OSCAR-PDGFR transmembrane fusion proteins were then subcloned into pMx puro using primers 5′-AGCTCGGATCCACTAGTAAC-3′ and 5′-GCTTCTCGAGCCAAAGCATGATGAGGATGA-3′ in frame with the cytoplasmic tail of the human CD3ζ chain, which was cloned using primers 5′-CTTGCTCGAGAGAGTGAAGTTCAGCAGGAG-3′ and 5′-TTGAGCGGCCGCATCCCCTGGCTGTTAGCGAG-3′. The following primers were used to clone murine DAP12 into pMx puro: 5′-CCTGGATTCTGGTGTCCAGTGCATATCTG-3′ and 5′-GCCGCGGCCGCGCATAGAGTGGGCTCATCTG-3′ and, OSCAR SP-S and SP-L, 5′-ACGGGGATCCCCCACCATGGTCCTGTCGCTGATAC-3′ and 5′-CTTCGCGGCCGCTCTCCAGGCAGTCTCTTCAG-3′.

NFAT-GFP reporter cell assays. Murine 2B4 NFAT-GFP reporter cells were a gift from Lewis Lanier, UCSF, San Francisco, California, USA (31). Transduced reporter cells were cultured on immobilized proteins and peptides for 24 hours at 37°C in a 5% CO_2 incubator prior to analysis of GFP expression by flow cytometry.

Calcium signaling. Monocytes were isolated using the Dynal Monocyte Negative Isolation Kit and stained with Fluo-3AM (3 μM for 30 minutes). Monocytes were serum starved for 2 hours before use. Cells were pipetted onto glass coverslips and coated with 10 μg/ml of either $(GPP)_{10}$ or OSC^{pep}. Monocytes were allowed to adhere for 10 minutes before unbound cells were removed by washing. Changes in intracellular calcium were recorded for 10 minutes with a laser scanning confocal microscope (Olympus) using a ×60 PLanApoN objective. Fluo-3 was excited at 488 nm and detection was at 510 to 570 nm.

Osteoclast cultures. Either 48- or 96-well tissue culture plates were coated with proteins and peptides, as described previously (29, 30). Unbound protein and peptides were removed by washing with PBS before blocking in a 5% CO_2 incubator in 2% BSA, followed by complete α-MEM (both for 1 hour at 37°C). Murine bone marrow was flushed from the tibias and femurs of 2- to 3-week-old mice, and stromal cells and ECM-free bone marrow precursors (9) were cultured as BMMs for 3 days in 100 ng/ml M-CSF (55) (±0.1 ng/ml TGF-β1 [Peprotech]) prior to osteoclast differentiation with 10 ng/ml M-CSF and either 30 ng/ml or 100 ng/ml RANKL (±0.1 ng/ml TGF-β1) in coated tissue culture plates. For human osteoclast cultures, peripheral blood monocytes were MACS sorted from either healthy donors or frozen ampoules of peripheral blood mononuclear cells isolated from patients with NH (56) deficient in either TREM-2 (patient NH2) or DAP12 (patient NH6) and cultured with 100 ng/ml RANKL and 30 ng/ml M-CSF (R&D Biosystems) on coated tissue culture plates, as previously described (14). The mean number of giant $TRAP^+$ cells with 3 or more nuclei from 3 wells was established.

Quantitative RT-PCR. DNAse-treated total RNA extracted from day 5 osteoclast cultures cultured on either immobilized BSA or OSC^{pep} was reverse transcribed using the SuperScript III Kit (Invitrogen), and quantitative PCR was performed on osteoclast-specific genes *TRAP*, *Ctsk*, *Calcr*, and *NFATc1*, as described previously (57).

Retroviral transductions. Plat-E cells were transfected with pMx puro retroviral constructs, and the resulting virus containing supernatants was used to infect either 2B4 NFAT-GFP reporter cells with selection of single-cell clones with 2.5 μg/ml puromycin or murine BMMs with 10 μg/ml puromycin selection, as described previously (58).

Cell culture staining techniques and imaging. In vitro osteoclast cultures were fixed with 4% PFA before staining for TRAP with a TRAP-staining kit (Sigma-Aldrich). Positive TRAP staining ($TRAP^+$) results in a deep red or dark purple histological stain. For fluorescence microscopy, PFA-fixed osteoclast cultures were permeabilized with 0.1% Triton in PBS for 10 minutes, before blocking in PBS/0.5% BSA and staining with Phalloidin–Alexa Fluor 488 and DAPI (Molecular Probes) to localize actin ring formation and nuclei, respectively. Bright-field or fluorescence images were captured using an Improvision OpenLab deconvolution microscope.

Mice and in vivo bone analysis. The genomic region of OSCAR was cloned from a 129/Sv mouse genomic lambda phage library by using a full-length OSCAR cDNA as probe. To make the gene targeting construct, long- and short-homology fragments amplified by PCR were ligated into the pPNT vector (59). The long-homology fragment was a 5.0-kb portion of the 3′ untranslated sequence of the *OSCAR* gene, and the short-homology fragment was a 1.0-kb portion of the intron 2 sequence of OSCAR. Homologous recombination in ES cells (59) produced a deletion of approximately 3.0 kb, containing the entire extracellular domain (exon 3 and 4) and transmembrane domain (exon 5) of OSCAR. The E14.1 ES cells were cultured on mouse embryonic fibroblast feeder layers in DMEM containing 15% fetal calf serum and 1,000 U of leukaemia inhibitory factor. The ES cells were electroporated with 50 mg linearized targeting vector using a Bio-Rad electroporator (220 V and 960 mF). Transfected cells were cultured with 200 mg/ml active G418 (GIBCO/BRL) and 0.2 mM Gancyclovir (Roche Laboratories) for 7 to 9 days. After selection, 1,000 colonies were picked and further analyzed by Southern blot. Four correctly targeted clones were obtained, and 2 of them were microinjected into blastocysts from C57BL/6 mice. Founders were bred with 129/Sv mice to test for germ-line transmission. C57BL/6 $Fcer1g^{-/-}$ and $DAP12^{-/-}$ mice have been described before (60). To generate $DAP12^{-/-}$ and $DAP12^{-/-}Oscar^{-/-}$ double-knockout mice, we first bred $DAP12^{-/-}$ to $Oscar^{-/-}$ mice to obtain $DAP12^{-/+}Oscar^{-/+}$ F1 mice. These were intercrossed, and offspring with appropriate genotypes were selected to establish $DAP12^{-/-}Oscar^{-/-}$ and $DAP12^{-/-}$ lines. Histomorphometric analyses of bone from 4-week-old mice were carried out essentially as described previously (9). For μCT analysis, the trabecular volume in the distal femoral metaphysis in 12-week-old mice was measured using a Scanco μCT40 Scanner (Scanco Medical AG). A threshold of 200 was used for evaluation of scans. All mice were born and bred under specific pathogen–free conditions.

Statistics. Statistical significance was determined using GraphPad Prism, version 4.0c. Statistical differences were determined by 2-tailed Student's *t* test (between 2 groups) and a 1-way ANOVA (among multiple groups). $P < 0.05$ was considered to indicate statistical significance.

Study approval. All human and animal studies were reviewed and approved by the Washington University in St. Louis human and animal studies committees. Informed consent was obtained from all subjects included in this study.

Acknowledgments

This work was funded by grants from the Wellcome Trust, the Medical Research Council, and the British Heart Foundation (to R.W. Farndale and J. Trowsdale); the Ministry of National Defense Foundation grant from the Korean Government (to J. Rho); and NIH grants (to Y. Choi and J. Lorenzo). A.D. Barrow is the recipient of a Marie Curie International Outgoing Fellowship from the EC framework programme (FP)7 and was awarded an international traveling fellowship from the Company of Biologists. M. Colonna is supported by NIH grant R01 HL097805. We thank Jim Kaufman (University of Cambridge) for critical reading of this manuscript.

Received for publication November 27, 2010, and accepted in revised form July 1, 2011.

Address correspondence to: Alexander David Barrow, Department of Pathology, University of Cambridge, Tennis Court Road, Cam-

bridge CB2 1QP, United Kingdom. Phone: 0044.0.1223.330248; Fax: 0044.0.1223.333875; E-mail: adb44@cam.ac.uk. Or to: Yongwon Choi, Department of Pathology and Laboratory Medicine, University of Pennsylvania School of Medicine, 421 Curie Blvd., Philadelphia, Pennsylvania 19104, USA. Phone: 215.746.6404; Fax: 215.573.0888; E-mail: ychoi3@mail.med.upenn.edu.

1. Geissmann F, Manz MG, Jung S, Sieweke MH, Merad M, Ley K. Development of monocytes, macrophages, and dendritic cells. *Science*. 2010; 327(5966):656–661.
2. Gordon S, Martinez FO. Alternative activation of macrophages: mechanism and functions. *Immunity*. 2010;32(5):593–604.
3. Martin TJ. Paracrine regulation of osteoclast formation and activity: milestones in discovery. *J Musculoskelet Neuronal Interact*. 2004;4(3):243–253.
4. Kong YY, et al. Activated T cells regulate bone loss and joint destruction in adjuvant arthritis through osteoprotegerin ligand. *Nature*. 1999; 402(6759):304–309.
5. Paloneva J, et al. Loss-of-function mutations in TYROBP (DAP12) result in a presenile dementia with bone cysts. *Nat Genet*. 2000;25(3):357–361.
6. Teitelbaum SL. Bone resorption by osteoclasts. *Science*. 2000;289(5484):1504–1508.
7. Kong YY, et al. OPGL is a key regulator of osteoclastogenesis, lymphocyte development and lymph-node organogenesis. *Nature*. 1999; 397(6717):315–323.
8. Lacey DL, et al. Osteoprotegerin ligand is a cytokine that regulates osteoclast differentiation and activation. *Cell*. 1998;93(2):165–176.
9. Koga T, et al. Costimulatory signals mediated by the ITAM motif cooperate with RANKL for bone homeostasis. *Nature*. 2004;428(6984):758–763.
10. Mocsai A, et al. The immunomodulatory adapter proteins DAP12 and Fc receptor gamma-chain (FcRgamma) regulate development of functional osteoclasts through the Syk tyrosine kinase. *Proc Natl Acad Sci U S A*. 2004;101(16):6158–6163.
11. Negishi-Koga T, Takayanagi H. Ca2+-NFATc1 signaling is an essential axis of osteoclast differentiation. *Immunol Rev*. 2009;231(1):241–256.
12. Ivashkiv LB. Cross-regulation of signaling by ITAM-associated receptors. *Nat Immunol*. 2009; 10(4):340–347.
13. Shinohara M, et al. Tyrosine kinases Btk and Tec regulate osteoclast differentiation by linking RANK and ITAM signals. *Cell*. 2008;132(5):794–806.
14. Cella M, Buonsanti C, Strader C, Kondo T, Salmaggi A, Colonna M. Impaired differentiation of osteoclasts in TREM-2-deficient individuals. *J Exp Med*. 2003;198(4):645–651.
15. Klunemann HH, et al. The genetic causes of basal ganglia calcification, dementia, and bone cysts: DAP12 and TREM2. *Neurology*. 2005;64(9):1502–1507.
16. Paloneva J, et al. DAP12/TREM2 deficiency results in impaired osteoclast differentiation and osteoporotic features. *J Exp Med*. 2003;198(4):669–675.
17. Merck E, et al. OSCAR is an FcRgamma-associated receptor that is expressed by myeloid cells and is involved in antigen presentation and activation of human dendritic cells. *Blood*. 2004; 104(5):1386–1395.
18. Kim N, Takami M, Rho J, Josien R, Choi Y. A novel member of the leukocyte receptor complex regulates osteoclast differentiation. *J Exp Med*. 2002; 195(2):201–209.
19. Collin-Osdoby P, Rothe L, Anderson F, Nelson M, Maloney W, Osdoby P. Receptor activator of NF-kappa B and osteoprotegerin expression by human microvascular endothelial cells, regulation by inflammatory cytokines, and role in human osteoclastogenesis. *J Biol Chem*. 2001;276(23):20659–20672.
20. Chow J, Chambers TJ. An assessment of the prevalence of organic material on bone surfaces. *Calcif Tissue Int*. 1992;50(2):118–122.
21. Miller SC, Bowman BM, Smith JM, Jee WS. Characterization of endosteal bone-lining cells from fatty marrow bone sites in adult beagles. *Anat Rec*. 1980;198(2):163–173.
22. Vanderwiel C. An ultrastructural study of the components which make up the resting surface of bone. *Metab Bone Dis Rel Res*. 1980;2(suppl):109–116.
23. Andersen TL, et al. A physical mechanism for coupling bone resorption and formation in adult human bone. *Am J Pathol*. 2009;174(1):239–247.
24. Hauge EM, Qvesel D, Eriksen EF, Mosekilde L, Melsen F. Cancellous bone remodeling occurs in specialized compartments lined by cells expressing osteoblastic markers. *J Bone Miner Res*. 2001;16(9):1575–1582.
25. Miller SC, Jee WS. The bone lining cell: a distinct phenotype? *Calcif Tissue Int*. 1987;41(1):1–5.
26. Gelse K, Poschl E, Aigner T. Collagens--structure, function, and biosynthesis. *Adv Drug Deliv Rev*. 2003;55(12):1531–1546.
27. Eriksen EF, Eghbali-Fatourechi GZ, Khosla S. Remodeling and vascular spaces in bone. *J Bone Miner Res*. 2007;22(1):1–6.
28. Farndale RW, Sixma JJ, Barnes MJ, de Groot PG. The role of collagen in thrombosis and hemostasis. *J Thromb Haemost*. 2004;2(4):561–573.
29. Raynal N, et al. Use of synthetic peptides to locate novel integrin alpha2beta1-binding motifs in human collagen III. *J Biol Chem*. 2006;281(7):3821–3831.
30. Konitsiotis AD, Raynal N, Bihan D, Hohenester E, Farndale RW, Leitinger B. Characterization of high affinity binding motifs for the discoidin domain receptor DDR2 in collagen. *J Biol Chem*. 2008; 283(11):6861–6868.
31. Arase H, Mocarski ES, Campbell AE, Hill AB, Lanier LL. Direct recognition of cytomegalovirus by activating and inhibitory NK cell receptors. *Science*. 2002;296(5571):1323–1326.
32. Paloneva J, et al. Mutations in two genes encoding different subunits of a receptor signaling complex result in an identical disease phenotype. *Am J Hum Genet*. 2002;71(3):656–662.
33. Helming L, et al. Essential role of DAP12 signaling in macrophage programming into a fusion-competent state. *Sci Signal*. 2008;1(43):ra11.
34. Otero K, et al. Macrophage colony-stimulating factor induces the proliferation and survival of macrophages via a pathway involving DAP12 and beta-catenin. *Nat Immunol*. 2009;10(7):734–743.
35. Peng Q, Malhotra S, Torchia JA, Kerr WG, Coggeshall KM, Humphrey MB. TREM2- and DAP12-dependent activation of PI3K requires DAP10 and is inhibited by SHIP1. *Sci Signal*. 2010;3(122):ra38.
36. Zou W, Reeve JL, Liu Y, Teitelbaum SL, Ross FP. DAP12 couples c-Fms activation to the osteoclast cytoskeleton by recruitment of Syk. *Mol Cell*. 2008;31(3):422–431.
37. Kindle L, Rothe L, Kriss M, Osdoby P, Collin-Osdoby P. Human microvascular endothelial cell activation by IL-1 and TNF-alpha stimulates the adhesion and transendothelial migration of circulating human CD14+ monocytes that develop with RANKL into functional osteoclasts. *J Bone Miner Res*. 2006;21(2):193–206.
38. Thesingh CW, Burger EH. The role of mesenchyme in embryonic long bones as early deposition site for osteoclast progenitor cells. *Dev Biol*. 1983; 95(2):429–438.
39. Masuyama R, et al. Vitamin D receptor in chondrocytes promotes osteoclastogenesis and regulates FGF23 production in osteoblasts. *J Clin Invest*. 2006;116(12):3150–3159.
40. Herman S, et al. Induction of osteoclast-associated receptor, a key osteoclast costimulation molecule, in rheumatoid arthritis. *Arthritis Rheum*. 2008; 58(10):3041–3050.
41. Zhu XW, Price NM, Gilman RH, Recarvarren S, Friedland JS. Multinucleate giant cells release functionally unopposed matrix metalloproteinase-9 in vitro and in vivo. *J Infect Dis*. 2007;196(7):1076–1079.
42. Levental KR, et al. Matrix crosslinking forces tumor progression by enhancing integrin signaling. *Cell*. 2009;139(5):891–906.
43. Ma G, et al. Paired immunoglobin-like receptor-B regulates the suppressive function and fate of myeloid-derived suppressor cells. *Immunity*. 2011; 34(3):385–395.
44. Barrow AD, Trowsdale J. You say ITAM and I say ITIM, let's call the whole thing off: the ambiguity of immunoreceptor signalling. *Eur J Immunol*. 2006; 36(7):1646–1653.
45. Mori Y, et al. Inhibitory immunoglobulin-like receptors LILRB and PIR-B negatively regulate osteoclast development. *J Immunol*. 2008;181(7):4742–4751.
46. van Beek EM, et al. Inhibitory regulation of osteoclast bone resorption by signal regulatory protein alpha. *FASEB J*. 2009;23(12):4081–4090.
47. Wu Y, Tworkoski K, Michaud M, Madri JA. Bone marrow monocyte PECAM-1 deficiency elicits increased osteoclastogenesis resulting in trabecular bone loss. *J Immunol*. 2009;182(5):2672–2679.
48. Barrow AD, Trowsdale J. The extended human leukocyte receptor complex: diverse ways of modulating immune responses. *Immunol Rev*. 2008;224:98–123.
49. Lebbink RJ, et al. Collagens are functional, high affinity ligands for the inhibitory immune receptor LAIR-1. *J Exp Med*. 2006;203(6):1419–1425.
50. Kim GS, et al. Association of the OSCAR promoter polymorphism with BMD in postmenopausal women. *J Bone Miner Res*. 2005;20(8):1342–1348.
51. Bouchon A, Facchetti F, Weigand MA, Colonna M. TREM-1 amplifies inflammation and is a crucial mediator of septic shock. *Nature*. 2001; 410(6832):1103–1107.
52. Barrow AD, et al. Cutting edge: TREM-like transcript-1, a platelet immunoreceptor tyrosine-based inhibition motif encoding costimulatory immunoreceptor that enhances, rather than inhibits, calcium signaling via SHP-2. *J Immunol*. 2004;172(10):5838–5842.
53. Kennedy J, et al. A molecular analysis of NKT cells: identification of a class-I restricted T cell-associated molecule (CRTAM). *J Leukoc Biol*. 2000; 67(5):725–734.
54. Angata T, Tabuchi Y, Nakamura K, Nakamura M. Siglec-15: an immune system Siglec conserved throughout vertebrate evolution. *Glycobiology*. 2007;17(8):838–846.
55. Takeshita S, Kaji K, Kudo A. Identification and characterization of the new osteoclast progenitor with macrophage phenotypes being able to differentiate into mature osteoclasts. *J Bone Miner Res*. 2000;15(8):1477–1488.
56. Kondo T, et al. Heterogeneity of presenile dementia with bone cysts (Nasu-Hakola disease): three genetic forms. *Neurology*. 2002;59(7):1105–1107.
57. Mao D, Epple H, Uthgenannt B, Novack DV, Faccio R. PLCgamma2 regulates osteoclastogenesis via its interaction with ITAM proteins and GAB2. *J Clin Invest*. 2006;116(11):2869–2879.
58. Lee SH, et al. v-ATPase V0 subunit d2-deficient mice exhibit impaired osteoclast fusion and increased bone formation. *Nat Med*. 2010;12(12):1403–1409.
59. Rho J, Gong S, Kim N, Choi Y. TDAG51 is not essential for Fas/CD95 regulation and apoptosis in vivo. *Mol Cell Biol*. 2001;21(24):8365–8370.
60. Turnbull IR, McDunn JE, Takai T, Townsend RR, Cobb JP, Colonna M. DAP12 (KARAP) amplifies inflammation and increases mortality from endotoxemia and septic peritonitis. *J Exp Med*. 2005;202(3):363–369.